

The signature of a double quantum-dot structure in the I-V characteristics of a complex system

L. Bitton, D. Radovsky, A. Cohen, A. Frydman, and R. Berkovits

*The Minerva Center, The Department of Physics,
Bar Ilan University, Ramat Gan 52900, Israel*

(Dated: November 14, 2018)

Abstract

We demonstrate that by carefully analyzing the temperature dependent characteristics of the I-V measurements for a given complex system it is possible to determine whether it is composed of a single, double or multiple quantum-dot structure. Our approach is based on the orthodox theory for a double-dot case and is capable of simulating I-V characteristics of systems with any resistance and capacitance values and for temperatures corresponding to thermal energies larger than the dot level spacing. We compare I-V characteristics of single-dot and double-dot systems and show that for a given measured I-V curve considering the possibility of a second dot is equivalent to decreasing the fit temperature. Thus, our method allows one to gain information about the structure of an experimental system based on an I-V measurement.

PACS numbers: 73.63.Kv; 73.23.Hk

Much of the study of charging effects in quantum systems has focused on a single-dot system, in which a metallic island is coupled to two metallic leads via tunnel junctions [1]. If the electron density is large enough so that the discrete energy level spacing is negligible compared to the other energy scales, the relevant scales are the thermal energy, $E_T = K_B T$, and the charging energy, $E_C = \frac{e^2}{C}$, where C is the capacitance of the dot. For low temperatures and small bias ($E_T < eV < E_C$), no current can flow through the dot leading to a Coulomb blockade in the I-V characteristic. An effective method to treat such a system is the orthodox theory [2, 3]. In this framework the quantum dot is represented by a Double Barrier Tunneling Junction (DBTJ) in which each junction is modeled as a resistor and a capacitor connected in parallel. For a given voltage, V , a distribution function, ρ , determines the probability at time t for the system to have N extra electrons on the island. Solving the master equation for ρ enables one to derive the current-voltage relation as a function of the tunneling rates. The orthodox model assumes that the tunneling events are sequential and an electron loses its phase coherence during a tunnel process, thus, quantum corrections are not taken into account [2, 3].

This approach has been very successful in analyzing the behavior of a single quantum dot. In many experimental systems, however, the exact structure is unknown. Even if a sample exhibits Coulomb-blockade-like features, one can not always be certain that only one simple quantum dot is involved in the transport process. An example for such a system is demonstrated in figure 1 which shows the I-V characteristic of a Co nanowire, $10\mu m$ long and $200nm$ wide [4]. The wire was evaporated on a step-edge structure [5] and was allowed to oxidize in atmosphere. It is seen that the I-V curve shows Coulomb-blockade-like behavior, presumably, due to the oxidation that gives rise to the formation of metallic islands separated by nanoconstrictions. However, a-priori it is impossible to know whether the structure consists of one dominant quantum dot, two dots or perhaps even more. A similar situation occurs in many experimental configurations and often it is desirable to find a way to determine the exact structure of the sample. In this paper we show that it is, in principle, possible to fit given I-V curves to both single and double-dot configurations using the orthodox model when the capacitance and resistance of the barriers as well as the temperature are treated as fit parameters. Nevertheless, since the temperature is usually well controlled in the experimental set up, it is possible to determine whether a system contains one or more quantum dots based on I-V measurements at a given temperature.

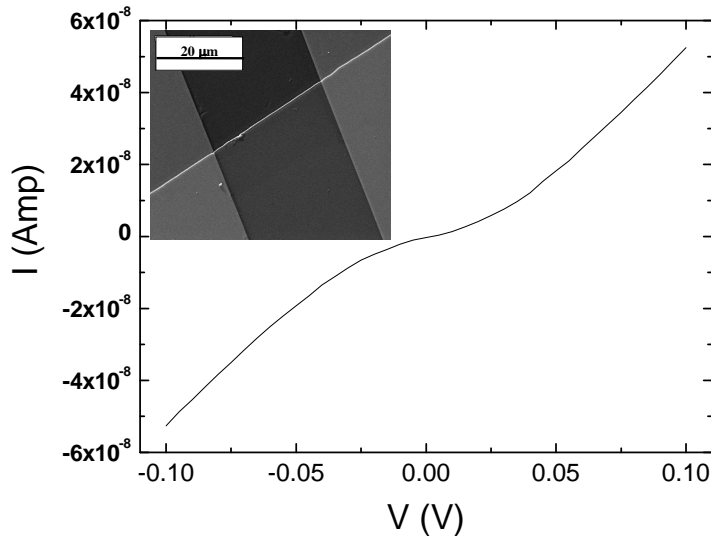


FIG. 1: I-V characteristic at $T=10\text{K}$ of a Co wire evaporated on a step-edge. The inset shows an SEM picture of the wire (white line) grown between two large Co electrodes (gray pads).

Most research studying the transport through double-dot system have taken into account the discrete energy spectrum in the dots [6, 7, 8]. In our approach, the more common case for metallic dots, i.e. discrete energy level spacing much smaller than $K_B T$, is considered.

The orthodox theory solution to the single dot (DBTJ) case is well known [2, 3]. Here we shall describe the double-dot case which contains three tunnel junctions and is named Triple Barrier Tunnel Junction (TBTJ). As in the DBTJ case, we assume that the tunneling coefficient is low and tunneling events are sequential and non-coherent, hence quantum interference effects are neglected. In our TBTJ model each of the three junctions $i=1,2,3$ is characterized by a tunneling resistance R_i and a capacitance C_i (see Fig. 2). The “state” of the system is determined by the number of excess electrons on each grain (n_1, n_2) . Similar to the case of DBTJ for $T=0$ the distribution function is sharply peaked for each voltage around a most probable state (n_1^*, n_2^*) . However, in contrast to the DBTJ case, one cannot determine this state analytically and a more complex method is required. Previous calculations on I-V characteristics of TBTJ systems [9, 10] overcame this difficulty by restricting the junction parameters (the resistance between the dots was assumed to be much higher dot-lead resistances), and the temperature was taken to be zero. We suggest an approach that allows one to calculate the distribution function in a general case without making any assumptions on the system. Moreover we calculate the probability value for any state, thus we can simulate the I-V curves for any given temperature.

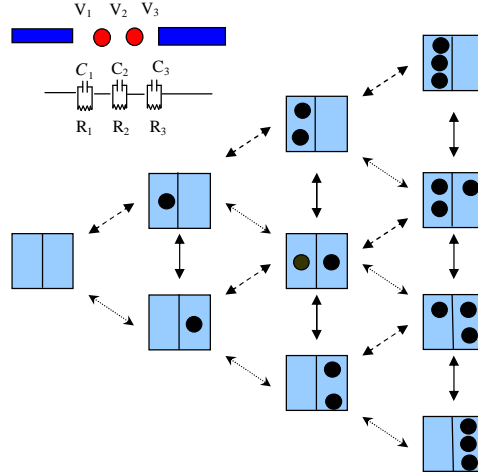


FIG. 2: A schematic illustration of a system through which three electrons are allowed to pass. Each box is divided to two parts where each denotes one dot. Each dot is allowed to contain 0-3 electrons. The arrows indicate a permitted tunneling between states. For the current calculation one has to sum over the transitions for a specific kind of arrow which are related to a specific junction: middle barrier (solid line), left barrier (dashed line) and right barrier (dotted line). The insert shows a schematic representation of a system composed of three tunnel junctions coupled in series. Each junction is characterized by a capacitance and resistance.

Applying voltage to a TBTJ system causes three different voltage drops V_i across the tunnel junctions i:

$$\begin{aligned}
 V_1 &= \frac{eC_2C_3V}{(C_1C_2 + C_2C_3 + C_3C_1)}, \\
 V_2 &= \frac{eC_1C_3V}{(C_1C_2 + C_2C_3 + C_3C_1)}, \\
 V_3 &= \frac{eC_1C_2V}{(C_1C_2 + C_2C_3 + C_3C_1)}.
 \end{aligned} \tag{1}$$

Accordingly, six tunneling rates have to be considered. Each tunneling rate depends

on the energy difference before and after the tunneling event and on the resistance of the relevant junction. The tunneling can be derived from Fermi's Golden rule:

$$\Gamma_{\pm k}^i = \frac{\Delta(E_{\pm k}^i)}{e^2 R_i (1 - \exp(-\Delta(E_{\pm k}^i)/k_\beta T))}, \quad (2)$$

where $\Gamma_{\pm k}^i$ is the electron tunneling rate on (+) or off (-) dot k across junction i . The energy differences, $E_{\pm k}^i$ can be derived by subtracting the electrostatic energy on the island after the tunneling event from that before the tunneling adding the gain in energy due to the voltage drop. The total energy differences due to tunneling of electrons from the dots to the leads are given by:

$$\Delta E_{\pm 1}^1 = \frac{(C_2 + C_3)[(Q_1 \pm e)^2 - Q_1^2]}{2(C_1 C_2 + C_2 C_3 + C_3 C_1)} \mp V_1, \quad (3)$$

$$\Delta E_{\pm 2}^3 = \frac{(C_1 + C_2)[(Q_2 \pm e)^2 - Q_2^2]}{2(C_1 C_2 + C_2 C_3 + C_3 C_1)} \mp V_3, \quad (4)$$

where $Q_1 = en_1, Q_2 = en_2$.

Taking into account the electrostatic energy differences of both the dots the energy difference due to tunneling of electrons from one dot to another is given by:

$$\begin{aligned} \Delta E_{\pm 1}^2 &= \frac{(C_2 + C_3)[(Q_1 \pm e)^2 - Q_1^2]}{2(C_1 C_2 + C_2 C_3 + C_3 C_1)} \\ &+ \frac{(C_1 + C_2)[(Q_2 \pm e)^2 - Q_2^2]}{2(C_1 C_2 + C_2 C_3 + C_3 C_1)} \mp V_3. \end{aligned} \quad (5)$$

For the TBTJ ρ is the probability to have n_1 and n_2 electrons on the first and second grain respectively, hence the master equation in a double-dot system is:

$$\begin{aligned} \frac{\partial \rho(V, n_1, n_2, t)}{\partial t} &= \rho(V, n_1 - 1, n_2, t) \Gamma_{+1}^1 + \rho(V, n_1 + 1, n_2, t) \Gamma_{-1}^1 \\ &+ \rho(V, n_1, n_2 - 1, t) \Gamma_{+2}^3 + \rho(V, n_1, n_2 + 1, t) \Gamma_{-2}^3 \\ &+ \rho(V, n_1 - 1, n_2 + 1, t) \Gamma_{+1}^2 + \rho(V, n_1 + 1, n_2 - 1, t) \Gamma_{-1}^2 \\ &- \rho(V, n_1, n_2, t) [\Gamma_{+1}^1 + \Gamma_{-1}^1 + \Gamma_{+1}^2 + \Gamma_{-1}^2 + \Gamma_{+2}^3 + \Gamma_{-2}^3]. \end{aligned} \quad (6)$$

In order to find the steady state solution of the distribution function we take $\frac{\partial \rho}{\partial t} = 0$. Solving this equation requires a constraint on the number of electrons permitted to pass

through the system. For a specific number of electrons n_e , there exists a specific number of states, N . In Fig. 2 we show a schematic drawing of the transitions between the charge configuration of a double-dot system allowing the addition of up to three electrons to the system.

For each state we manipulate the master equation, thus achieving a system of N linear equations, where N is the number of states. This system is described by the formula:

$$\Gamma \cdot \vec{\rho} = 0, \quad (7)$$

where Γ is a rate matrix and $\vec{\rho}$ is the states vector. The sum over all the probabilities should be one. For simplicity we add the normalization condition in the last row of the rate matrix. Thus, the previous equation takes the form:

$$\begin{bmatrix} -(\Gamma_{+1}^1 + \Gamma_{+2}^3) & \Gamma_{-2}^3 & \Gamma_{-1}^1 \dots & & \\ \Gamma_{+2}^3 & -(\Gamma_{+2}^3 + \Gamma_{+1}^1 + \Gamma_{+1}^2 + \Gamma_{-2}^3) & \Gamma_{-1}^2 \dots & & \\ \Gamma_{+1}^1 & \Gamma_{+1}^2 & -(\Gamma_{+1}^1 + \Gamma_{-1}^2 + \Gamma_{-1}^1 + \Gamma_{+2}^3) \dots & & \\ \vdots & \ddots & & & \\ 1 & 1 & 1 \dots & & \end{bmatrix} \begin{bmatrix} \langle 0, 0 \rangle \\ \langle 0, 1 \rangle \\ \langle 1, 0 \rangle \\ \vdots \\ \langle n_e, 0 \rangle \end{bmatrix} = \begin{bmatrix} 0 \\ 0 \\ 0 \\ \vdots \\ 1 \end{bmatrix} \quad (8)$$

By solving this numerically we obtain the distribution function and the vector $\vec{\rho}$. The current for a given voltage is derived by summing over all the possibilities for an electron to pass through a certain junction:

$$I(V) = \sum_{k,i,n_1,n_2} C_{\pm k}^i \cdot \rho(V, n_1, n_2) \cdot \Gamma_{\pm k}^i(n_1, n_2), \quad (9)$$

where $C_{\pm k}^i = \pm$ is determined by the direction of the tunneling.

The results presented in this paper are obtained for a system of up to 4 electrons tunneling through the dot. In order to verify that this does not lead to a considerable loss of information we plot the numerical I-V characteristics of a typical TBTJ for 1 to 4 tunneling electrons in Fig. 3. It can be seen that the curves for 3 and 4 electrons practically coincide for the relevant voltage regime, hence we conclude that further increasing the number of electrons would not have a noticeable effect on the I-V characteristics.

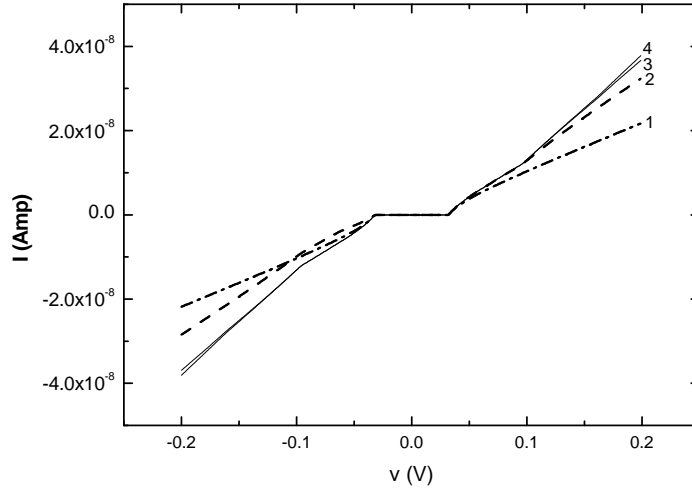


FIG. 3: I-V curves for the TBTJ model $T=0K$, $C_1 = C_2 = C_3 = 5 \cdot 10^{-18}F$, $R_1 = R_2 = R_3 = 1 \cdot 10^6\Omega$. Each number in the graph indicates the number of electrons passing through the system. Curves 3 and 4 which corresponds to three and four electrons are, for all practical purposes, identical (at least in the range of the Coulomb Blockade).

Once more than two barriers are considered the system's parameter space (i.e., possible values of R_i, C_i) becomes large. It is helpful then to gain some information out of the general properties of the I-V curve. In this paper we shall concentrate on the simplest case of symmetric I-V curves with no prominent staircase features, which are surprisingly common in the experiments that are discussed later. Since in the Coulomb blockade range the case for which R_1, C_1 differs much from R_3, C_3 results in a non-symmetric I-V curve and in some cases leads to staircases with different widths and heights, we will only consider cases for which R_1, C_1 is similar to R_3, C_3 . Another crucial factor for the I-V characteristics are the parameters of the middle barrier (R_2, C_2). Choosing the parameters of the middle barrier significantly different than the other barriers results in I-V curves that show more prominent staircase structure. In Fig. 4. we compare the I-V curves for the three cases discussed above. The first case in which the parameters of the barriers are significantly different shows a pronounced non-symmetric I-V curve. In the second case, for which $R_1, C_1 = R_3, C_3 \neq R_2, C_2$, the I-V curve shows prominent staircase jumps. On the other hand for the case in which all barriers are equal the I-V curve is symmetric and smooth.

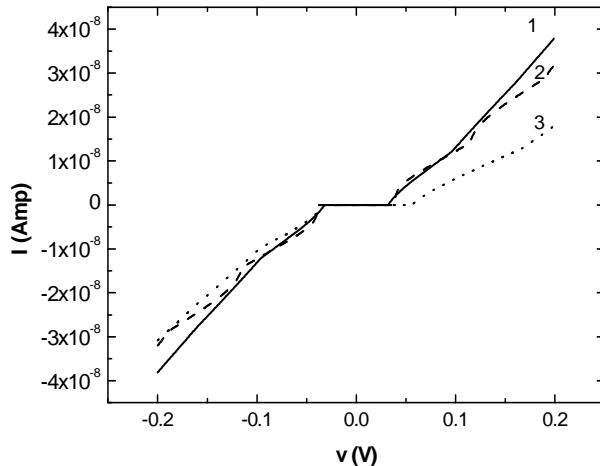


FIG. 4: Theoretical I-V curves at $T=0\text{k}$ for three cases. Curve 1 is the curve obtained for a pure symmetric system with the parameters $C_1 = C_2 = C_3 = 5 \cdot 10^{-18}F$, $R_1 = R_2 = R_3 = 1 \cdot 10^6\Omega$. Curve 2 was obtained on a system in which the parameters of middle barrier differ from rest barriers: $C_1 = C_3 = 7 \cdot 10^{-18}F$, $R_1 = R_3 = 1 \cdot 10^5$, $C_2 = 3 \cdot 10^{-18}$, $R_2 = 4 \cdot 10^6\Omega$. This results in prominent staircases. Curve 3 shows non-symmetric behavior where the dot-lead barriers are not equal: $C_1 = C_2 = 5 \cdot 10^{-18}F$, $R_1 = R_2 = 1 \cdot 10^6$, $C_3 = 2 \cdot 10^{-18}\Omega$, $R_3 = 2 \cdot 10^6\Omega$

We demonstrate the effectiveness of our analysis in determining the structure of a complex system by applying it to Co nanowires such as that depicted in Fig. 1. Fig. 5 shows the experimental results and the numerical fits of I-V characteristics of a typical nanowire taken at different temperatures. We used the orthodox theory to fit these data using DBTJ and TBTJ models. For the DBTJ we were able to obtain reasonable fits only using much higher temperatures than those of the experiment. Moreover, the ratio between the measured and calculated temperatures increased with T . Using our TBTJ calculation we were able to fit the data using the correct measurement temperatures [12]. This remarkable agreement for the different temperatures reinforces our confidence in the validity of the two-dot model to this experimental system. The diameters of the metallic islands according to our fit are found to be $\sim 30\text{nm}$. This is a reasonable value since it is close to the width of the wire.

We have applied this analysis to other wires. In some cases, even the TBTJ model yields good fits only for temperatures much higher than the experimental T . We suspect that these samples contain a larger number of islands for which a model that takes into account four

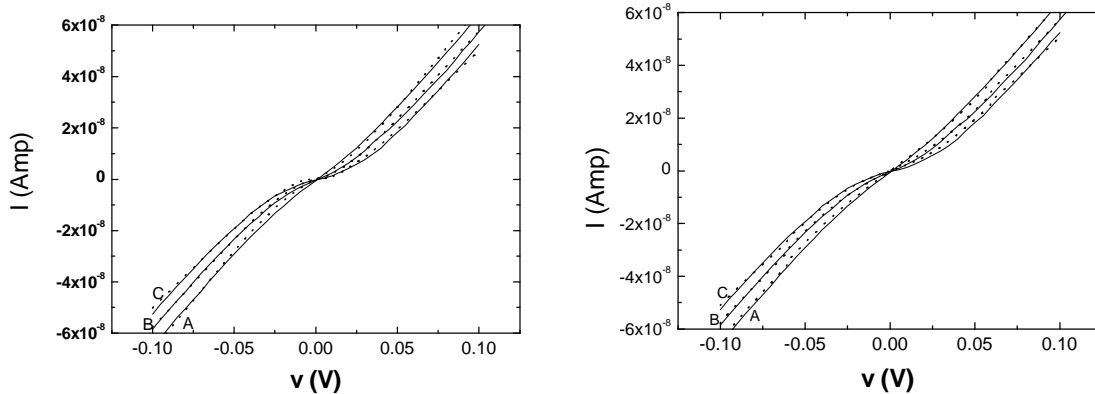


FIG. 5: DBTJ (right) and TBTJ (left) theoretical fits (dashed lines) to experimental I-V experimental curves (solid lines) for Co nanowire samples measured at 10K (A), 20K (B), and 30K (C). The fitting parameters for DBTJ: $R_1 = R_2 = 7 \cdot 10^5 \Omega$, $C_1 = C_2 = 4 \cdot 10^{-18} F$, $T=50K$ (A), 65K (B), 90K (C), for TBTJ: $R_1 = R_2 = R_3 = 4 \cdot 10^5 \Omega$, $C_1 = C_2 = C_3 = 1.55 \cdot 10^{-17} F$, $T=10K$ (A), 20K (B), 30K (C).

or more tunnel junctions is required.

Another complex system in which this analysis method may prove useful is a disordered granular sample. In such a system the geometrical structure may be known but the precise elements that dominate the transport are unidentified. We applied our analysis to a 400nm sample of 20–40nm grains placed on an insulating substrate and separated by a few nm of an insulating matrix. Though the sample contains about 400 grains, not all of them participate in the transport due to the hopping nature of the electric conductivity. Actually, it has been shown [11] that for low temperatures the transport is dominated by hopping through one or two grains. I-V characteristics of such a system show highly non-ohmic behavior that can be interpreted as signs for charging effects. Fig. 6. shows an I-V curve taken at $T = 6K$ together with fits to DBTJ and TBTJ models. Again, we were not able to fit the results to a single dot system without increasing the fitting temperature considerably. Using the TBTJ model, on the other hand, we were able to obtain a very good fit for $T = 6K$. From the fitting parameters we find that the diameter of the grains is about 40 nm, which is in

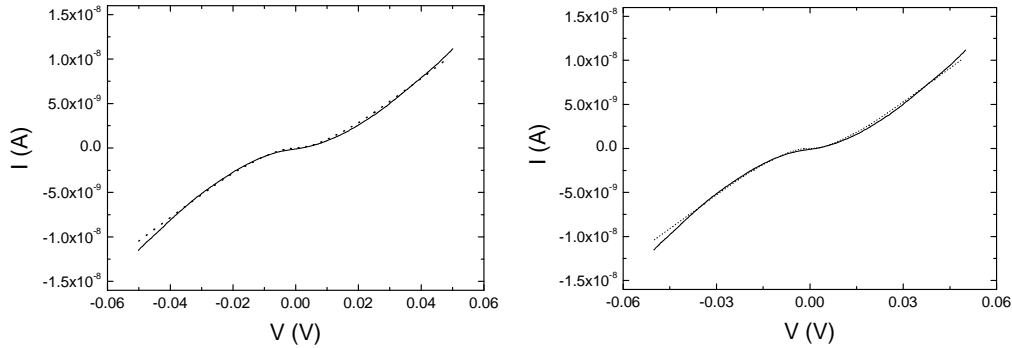


FIG. 6: Experimental results (solid lines) and theoretical fits (dashed lines) for the I-V characteristics of the granular systems. The left panel is the fit for the DBTJ at $T = 30K, C_1 = C_2 = 5 \cdot 10^{-18} F, R_1 = R_2 = 1.55 \cdot 10^6 \Omega$. The right panel is for the TBTJ at $T = 6K, C_1 = C_2 = C_3 = 2.8 \cdot 10^{-17} F, R_1 = R_2 = R_3 = 1 \cdot 10^6 \Omega$

accordance with AFM pictures obtained on these systems.

Both examples demonstrate that for a given experimental I-V curve, using the TBTJ model had a similar effect to that of using a DBTJ with higher temperature. This can be expected since the voltage drop in the Coulomb blockade regime is divided to the contributions of the two dots, each one contributing an energy which has to be compared to $K_B T$. Thus, the measurement temperature can be an important tool for determining the number of dots in a complex Coulomb blockade system. For further confirmation of the analysis it is recommendable to acquire I-V curves for different temperatures and repeat the procedure as demonstrated in Fig. 5.

As previously discussed, since the typical experimental I-V curves considered in this paper were symmetric and had no pronounced staircases, we choose all barrier parameters to be equal in the fitting procedure. The assumption that all R_i s and C_i s in the experimental structures are identical is clearly unrealistic. Nevertheless, we find that a finite temperature smears the difference between barriers which exhibit similar parameters. The effect of temperature is demonstrated in Fig. 7 where the TBTJ I-V curves for two different values of the middle barrier parameters ($R_2, C_2 = R_1, C_1 = R_3, C_3$ and $R_2, C_2 \neq R_1, C_1 = R_3, C_3$) at zero temperature and at $T = 6K$ are presented. At zero temperature there is a clear staircase structure for the latter case. At $T = 6K$, on the other hand, the staircase struc-

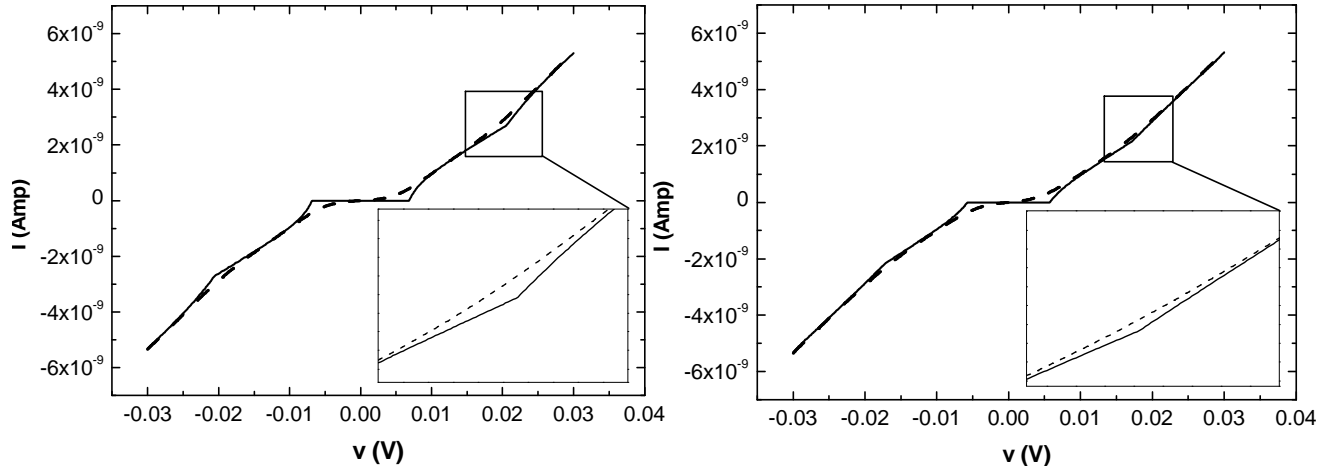


FIG. 7: Theoretical results for TBTJ at $T=0\text{K}$ (solid lines) and at $T=6\text{K}$ (dotted lines). The left panel is at $C_1 = C_3 = 2.8 \cdot 10^{-17} F$, $R_1 = R_3 = 5 \cdot 10^5 \Omega$, $R_2 = 2 \cdot 10^6 \Omega$, $C_2 = 2 \cdot 10^{-17}$. The right panel is for the total symmetric case: $C_1 = C_2 = C_3 = 2.8 \cdot 10^{-17} F$, $R_1 = R_2 = R_3 = 1 \cdot 10^6 \Omega$. One can notice that the staircases in the left panel are more prominent than in right panel and the dotted lines at both cases smears out the staircases.)

ture is smeared and the I-V curve is similar for both identical and non-identical barriers. Hence, measured I-V curves cannot determine the precise parameters of the barriers for the experimental realizations depicted in Figs. 5 and 6 and the best we can do is to estimate the barrier parameters to be roughly equal. For a more exact evaluation of the barrier parameters additional measurements at lower temperatures are required.

In summary, we propose that by analyzing the I-V characteristics one may identify systems which are more complicated than the conventional single-dot-double-barrier system although no former knowledge of the system is assumed. This enables to determine the geometrical structure of a complex quantum system. In the current work we have implemented our approach to identifying two-dot-triple-barrier configuration. Future work should

focus on extending this method to apply to more complex systems and, eventually, to find a way to determine the precise number of dots in an experimental system. This research was supported by the Israeli Science Foundation (grants number 326/02-3, 877/04).

-
- [1] For comprehensive reviews see U. Meirav and E.B. Foxman, *Semicond. Sci. Technol.* **11**, 255 (1996); Y. Alhassid, *Rev. Mod. Phys.*, **72**, 895 (2000).
 - [2] D. V. Averin and K. K. Likharev, "Mesoscopic Phenomena in Solids" p.169, edited by B.L. Altshuler, P.A.Lee, and R.A. Webb, Elsevier, Amsterdam, (1991).
 - [3] M. Amman, R. Wilkins et. al, *Phys. Rev.* **B43**, 1, 1146 (1991).
 - [4] D. Radovsky, A. Frydman and R. Berkovits, to be published.
 - [5] D. E. Prober, M. D. Feuer and N. Giordano, *Appl. Phys. Lett.* **37**, 94 (1980).
 - [6] V. N. Golovach and D. Loss, *Phys. Rev.* **B69**, 245327 (2004).
 - [7] J. R. Petta, A. C. Johnson, C. M. Marcus, M. P. Hanson and A. C. Gossard, *Phys. Rev. Lett.* **93**, 186802 (2004).
 - [8] N. C. van der Vaart, S. F. Godijn, Y. V. Nazarov, C. J. P. M. Harmans and J. E. Mooij, *Phys. Rev. Lett.* **74**, 4702 (1995).
 - [9] E. Bar-Sadeh , Y. Goldstein, C. Zhang, H. Deng, B. Abeles and O. Millo, *Phys. Rev.* **B50**, 8961 (1994).
 - [10] E. Bar-Sadeh , Y. Goldstein, M. Wolovelsly, D. Porath, C. Zhang, H. Deng, B. Abeles and O. Millo, *J. Vac. Sci Technol. B* **13(3)**, 1084 (1995).
 - [11] H. Vilchik, A Frydman and R. Berkovits, *Physica Status Solidi*, in press.
 - [12] In the fit we included a slight temperature dependence of the resistances as obtained in the experiment.